# Intermediate quantum maps for quantum computation

O. Giraud and B. Georgeot
*Laboratoire de Physique Théorique, UMR 5152 du CNRS, Université Paul Sabatier, 31062 Toulouse Cedex 4, France*
(Received 29 April 2005; published 7 October 2005)

We study quantum maps displaying spectral statistics intermediate between Poisson and Wigner-Dyson. It is shown that they can be simulated on a quantum computer with a small number of gates, and efficiently yield information about fidelity decay or spectral statistics. We study their matrix elements and entanglement production and show that they converge with time to distributions which differ from random matrix predictions. A randomized version of these maps can be implemented even more economically and yields pseudorandom operators with original properties, enabling, for example, one to produce fractal random vectors. These algorithms are within reach of present-day quantum computers.

DOI: 10.1103/PhysRevA.72.042312 PACS number(s): 03.67.Lx, 03.67.Mn, 05.45.Mt

The study of quantum information has attracted more and more interest from the scientific community in the recent past. Quantum communication and quantum computation have been shown to be deeply different from their classical counterparts. Algorithms have been built showing that quantum computers can outperform classical devices for some problems [1]. In particular, quantum mechanical systems can be simulated much faster on a quantum computer [2]. An especially congenial class of models corresponds to quantum maps. They can display complex dynamics, but can be described by simple evolution operators. It has been shown that the quantum baker's map [3], the quantum kicked rotator [4], and the quantum sawtooth map [5] can be simulated efficiently on a quantum computer. Still, even the simplest models are difficult to implement on the small-size quantum computers experimentally available, and only the quantum baker's map has been implemented to date with three qubits [6]. General algorithms have been proposed to probe phase space distributions [7], fidelity decay [8], form factors [9], or localization length [10] of such maps. Quantum maps have been also used as test grounds to study the production of entanglement in quantum systems [11]. Very recently, they have been used as models to build pseudorandom operators which can be efficiently implemented on quantum computers [12].

The models envisioned so far correspond mostly to chaotic maps, where the most complex behavior is expected to manifest itself, and eigenvalue statistics are close to those of the Wigner-Dyson ensembles of random matrix theory (RMT). Some integrable maps, which are expected to follow Poissonian statistics, have been also studied. However, it has been observed recently that some systems obey *intermediate statistics*, characterized by a level repulsion and a Poisson-like behavior at long distance in energy spacings. They can be modeled by the so-called semi-Poisson statistics [14] for which correlation functions can be explicitly calculated, giving energy level spacing distributions $P_\beta(s) \propto s^\beta e^{-(\beta+1)s}$. Such distributions have been first observed at the Anderson metal-insulator transition for electrons in disordered systems [13], and later in pseudointegrable systems [14] or in certain diffractive billiards [15]. They are usually associated with fractal properties of eigenstates.

In this paper, we study from the viewpoint of quantum computation a one-parameter family of quantum maps recently introduced [16]. They can be expressed in a particularly simple way, yet the spectral statistics display a wide range of semi-Poisson distributions depending on the value of the parameter. We first show that such maps can be simulated efficiently on a quantum computer and can be implemented with a remarkably small number of qubits and quantum gates. They are therefore good candidates for simulation on small-size quantum computers that will be built in the near future. In particular, they represent an ideal test ground for algorithms proposed in recent years which aim at measuring the form factor or the fidelity decay using only one qubit of quantum information. Indeed, the maps we study present a natural example where such algorithms can give results richer than in standard quantum chaotic systems for which random matrix theory applies. The properties of these maps being intermediate between chaos and integrability, we study how this translates in the matrix element distributions and the entangling power. At last, we show that a certain generalization of these maps which corresponds to a new ensemble of random matrices with semi-Poisson statistics recently proposed in [17] can be implemented even more efficiently on a quantum computer. They can be used as a way to produce a family of pseudorandom operators with new properties related to fractal behavior. We note that different distributions interpolating between Poisson and Wigner-Dyson, built from a partial randomization procedure, were studied in [18]. In our case, the intermediate distributions are of a completely different nature and furthermore have a more physical basis since they arise naturally in various quantum systems.

We start with the classical map defined by $\bar{p}=p+\alpha$ (mod 1); $\bar{q}=q+2\bar{p}$ (mod 1) where $(p,q)$ is the pair of conjugated momentum (action) and angle variables, and the bars denote the resulting variables after one iteration of the map. This map covers a wide range of dynamical behaviors depending on the value of the parameter $\alpha$. When $\alpha$ is irrational, it is uniquely ergodic but not mixing, while for rational $\alpha$ it reduces to an interval-exchange map (pseudointegrable dynamics) and for $\alpha=0$ it is trivially integrable (see [16] and references therein). The quantization of this map yields a

 

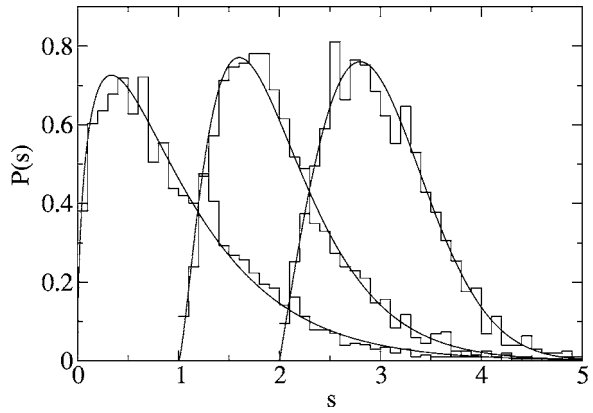


FIG. 1. Nearest-neighbor distribution of eigenvalues of $\hat{U}$ for $N=2^{12}$ and from left to right $\alpha=1/3$, $\alpha=1/5$, $\alpha=(1+\sqrt{5})/2$. Data are taken from the dissymmetrized spectra of $\alpha$ and $1-\alpha$. Distribution corresponding to $\alpha=1/5$ [respectively $\alpha=(1+\sqrt{5})/2$] is shifted by 1 (respectively 2) along the $s$ axis. The solid curves from left to right correspond to semi-Poisson with $\beta=1/2$, $\beta=3/2$, and COE.

unitary evolution operator which can be expressed in momentum space by the $N\times N$ matrix

$$U_{pp'}=\frac{\exp(-2i\pi p'^2/N)[1-\exp(2i\pi N\alpha)]}{1-\exp[2i\pi(p-p'+N\alpha)/N]}$$

[16], or alternatively in operator notation $\hat{U}=e^{-2i\pi\hat{p}^2/N}e^{2i\pi\alpha\hat{q}}$. For generic irrational $\alpha$, the spectral statistics of $\hat{U}$ are expected to follow RMT (in this case COE). For rational $\alpha=a/b$, a variety of different behaviors are observed [16]. In particular, it is conjectured from [17] that for $aN=\pm 1$ (mod b) the statistics of eigenvalues is of the semi-Poisson type $P_\beta(s)$ with parameter $\beta=b/2-1$. This can be checked in Fig. 1 where the statistics of eigenvalues is plotted for different values of $\alpha$ [for $N=0$ (mod 4) there is an additional symmetry $US=SU$, where $S_{qq'}=(-1)^q\delta_{qq'}$; each half of the spectrum should be considered separately [16]]. Thus $\hat{U}$ gives a set of quantum maps with statistics corresponding to natural intermediate distributions between Poisson and RMT, in a controllable manner.

The map $\hat{U}$ can be implemented efficiently on a quantum computer. Indeed, the use of the quantum Fourier transform (QFT) allows one to switch from position to momentum representation. More precisely, for one iteration of $\hat{U}$ on an $N$-dimensional Hilbert space with $N=2^{n_q}$, one first implements $\exp(2i\pi\alpha\hat{q})$, which is diagonal in the $q$-representation. This can be done efficiently using the binary decomposition of $q$: if $q=\Sigma_{j=0}^{n_q-1}q_j2^j$, then $\exp(2i\pi\alpha\hat{q})$ corresponds to the application of the $n_q$ one-qubit gates $|0\rangle\rightarrow|0\rangle$, $|1\rangle\rightarrow\exp(2i\pi\alpha 2^j)|1\rangle$. Then by using a QFT one can shift from $q$ to $p$ representation, using $n_q(n_q+1)/2$ gates. In this representation, the second operator $e^{-2i\pi\hat{p}^2/N}$ is diagonal. If $p=\Sigma_{j=0}^{n_q-1}p_j2^j$, then $\exp(-2i\pi p^2/N)=\Pi_{j_1,j_2}\exp(-2i\pi p_{j_1}p_{j_2}2^{j_1+j_2}/N)$. To simulate it, one needs $n_q^2$ two-qubit gates applied to each qubit pair $(j_1,j_2)$, keeping the states $|00\rangle,|01\rangle,|10\rangle$ unchanged while $|11\rangle\rightarrow\exp(-2i\pi 2^{j_1+j_2}/N)|11\rangle$. Then a QFT brings back the wave function to the $q$ representation. In total, the evolution requires $2n_q^2+2n_q$ gates to be implemented, of which $2n_q^2-n_q$ are two-qubit gates. This is less than any other map proposed to date (including the sawtooth map [5]), except the quantum baker's map, which has already been implemented [6].

The algorithm above can be used as a subroutine of other algorithms which aim at measuring quantum-mechanical quantities, with the attractive feature that it makes them very economical since the map evolution needs remarkably little quantum gates. One can, for example, probe Wigner and Husimi phase space distribution functions [7], or investigate fidelity decay in the presence of perturbation [8]; the fact that these maps correspond to spectral statistics intermediate between Wigner-Dyson and Poisson should translate into specific properties for these quantities. It has also been proposed to use a quantum computer to differentiate between quantum chaos and integrability by evaluating the form factor at short times [9]. In our case, the same algorithm can give much more information. The method in [9] adds one probe qubit to the system, performs $U^n$, and uses two additional one-qubit gates to transfer the trace of $U^n$ to the probe qubit. Using such scattering circuits, real and imaginary parts of $\mathrm{Tr}\,U^n/N$ correspond to expectation values of Pauli operators for the probe qubit. For COE or CUE, this quantity is of order $1/N$ for small $n$. In the case of intermediate statistics ($\alpha=a/b$), one expects $\langle\mathrm{Tr}\,U^n\rangle_n\sim\kappa\sqrt{N}$, where the average is taken over the first iterates of $U$. The form factor at short times is then given by $|\kappa|^2$. In order to get the value of $\kappa$ with enough precision, one needs a number of quantum measurements of order $N$ (the number of values of $n$ to average over depends only on $b$ [16] and does not vary with $N$). This implies a quadratic gain over classical computation. For $N=0$ (mod 4), in order to dissymmetrize the spectrum, one additionally has to perform the evolution of $SU^n$ (this only requires one extra controlled-phase gate), and the difference between the traces of $U^n$ and $SU^n$ gives the required quantity. Using this algorithm for large $N$ enables one to probe the form factor at increasingly short times and check the semiclassical conjectures [16]. The value of $|\kappa|^2$ also yields the level compressibility, which controls the behavior of the spectral number variance at infinity. It is possible that an exponential gain can be obtained through investigation of the fidelity decay [8]. We note that the fidelity decay can be explicitly related to the form factor [19]. Both quantities can be probed using deterministic quantum computation with one single pseudopure bit [20], which together with the small number of gates needed should make these simulations very attractive for NMR quantum computation.

It is instructive to study the entangling power of these maps. Indeed, entanglement is a key resource for quantum information [1]. Quantum chaotic evolutions have been shown to generate entanglement distributions similar to the predictions of RMT [11]. The entanglement can be measured by the average bipartite entanglement between one qubit and the rest of the system $Q=2-(2/n_q)\Sigma_{k=1}^{n_q}\mathrm{Tr}\,\rho_k^2$, where $\rho_k$ is the density operator corresponding to the $k$th qubit after having traced out the rest [21]. Figure 2 displays the distribution of matrix elements and $Q$ for the column vectors of $U^n$ for large

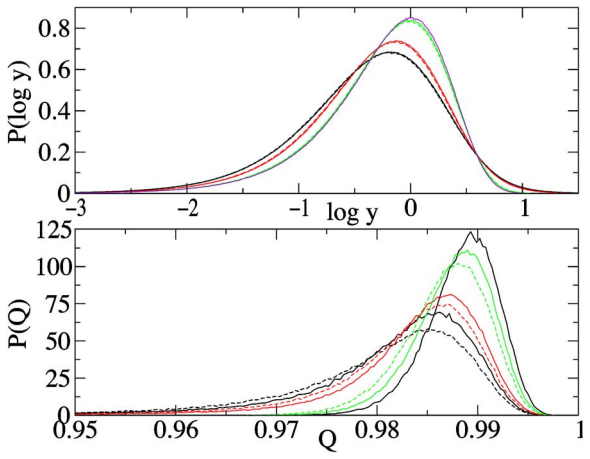


FIG. 2. (Color online) Distributions of matrix element (top) and $Q$ of column vectors (bottom) for iterates $\hat{U}^n$ of $\hat{U}$ for $N=2^9$, in $p$ representation. Matrix elements $x$ are rescaled by $y=N|x|^2$. Only one symmetry class of $S$ is taken. From lowest to topmost curve: black is $\alpha=1/3$, red is $\alpha=1/5$, green is $\alpha=(1+\sqrt{5})/2$, and purple is CUE. Full lines are averaged over $10^5 \leqslant n < 10^5+1000$, dashed lines are averaged over $1000 \leqslant n < 2000$ (top) and $2000 \leqslant n < 3000$ (bottom). Logarithms are decimal.

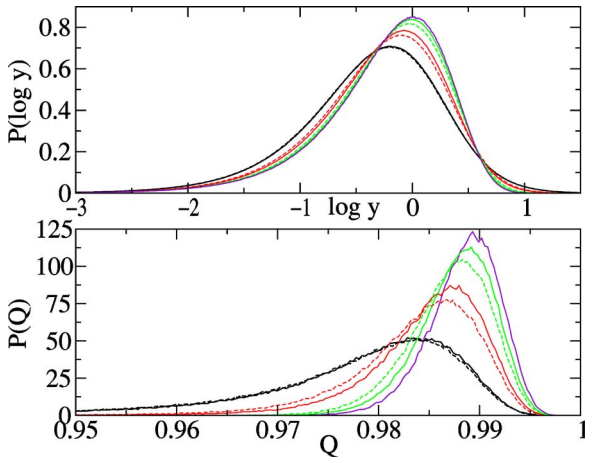


FIG. 3. (Color online) Same as Fig. 2 for iterates of ISRM, for $N=2^8$ (nonsymmetric case). Averages are made over 1000 disorder realizations at $n=10^5$ (full lines), $n=1000$ (dashed lines, top), and $n=2000$ (dashed lines, bottom). Logarithms are decimal.

$n$. It is compared with the RMT prediction computed numerically from the parametrization method of [22]. For irrational $\alpha$, the spectral statistics follow COE, but both matrix element and $Q$ distributions converge to CUE predictions. For values of $\alpha$ with intermediate statistics, there is a convergence to a distribution different from CUE predictions. This holds in $p$ representation: in $q$ representation both quantities converge to CUE predictions (data not shown). In all cases the convergence is faster for matrix elements than for $Q$; the convergence rate is similar to what is obtained for chaotic maps [11].

In [12], pseudorandom operators inspired by quantum chaotic maps were built which efficiently create entanglement and matrix element distributions close to RMT. In our case, it is possible to construct ensembles of intermediate statistics random matrices (ISRM) based on the quantum map $\hat{U}$ [17]. The procedure consists in replacing $e^{-2i\pi\hat{p}^2/N}$ in $\hat{U}$ by the diagonal matrix (in $p$ representation) $(e^{i\Phi_p}\delta_{pp'})$, where $\Phi_p$ are random variables either independent ("nonsymmetric case") or verifying $\Phi_{N-p}=\Phi_p$ ("symmetric case"). General arguments [17] indicate that for $\alpha$ irrational eigenvalue statistics for ISRM follow COE (symmetric case) or CUE (nonsymmetric case). For rational $\alpha=a/b$, and matrix size $N\to\infty$ obeying $aN=\pm 1$ (mod b), eigenvalue statistics follow the semi-Poisson prediction with $\beta=b-1$ (nonsymmetric case) or $\beta=b/2-1$ (symmetric case). These ISRM can be implemented on a quantum computer, actually more economically than $\hat{U}$. The only difference with the algorithm simulating $\hat{U}$ consists in the replacement of $e^{-2i\pi\hat{p}^2/N}$ by $(e^{i\Phi_p}\delta_{pp'})$. This operator multiplies each basis state $|p\rangle$ by a Gaussian random phase. It can be simulated by choosing $n_q+n_s$ independent and uniformly distributed random angles $\phi_k$, with $1 \leqslant k \leqslant n_q$, and $\phi'_k$, $1 \leqslant k \leqslant n_s$, for some integer $n_s$. Applying the controlled NOT and rotation operators $\Pi_{k=n_s}^{1}\mathrm{CNOT}_{i_k,j_k}\Pi_{k=1}^{n_s}[R_{j_k}(\phi'_k)\mathrm{CNOT}_{i_k,j_k}]\Pi_{k=1}^{n_q}R_k(\phi_k)$ multiplies each basis state by a random variable $\pm\phi_1\pm\phi_2\pm\cdots\pm\phi'_{n_s-1}\pm\phi'_{n_s}$, which for large $n_s$ tends to a Gaussian random variable. Here $R_j(\phi)=\exp(i\phi\sigma_j^z/2)$ is the rotation on the $j$th qubit by an angle $\phi/2$, $\mathrm{CNOT}_{i,j}$ (controlled NOT) is the bit-flip on the $j$th qubit conditioned by the $i$th qubit, and the $i_k$ and $j_k$ are chosen randomly between 1 and $n_q$. This transformation requires $(3n_s+n_q)$ gates instead of the $n_q^2$ gates needed for $e^{-2i\pi\hat{p}^2/N}$. In practice, $n_s$ is taken proportional to $n_q$, and the simulation requires in total $n_q^2-n_q+2n_s$ two-qubit gates and $4n_q+n_s$ one-qubit gates. This is quite close to what is needed to simulate the quantum baker's map already implemented [6], thus ISRM should be implementable as well in present-day quantum computers.

The latter algorithm can be used to generate pseudorandom operators having original properties. Figure 3 shows

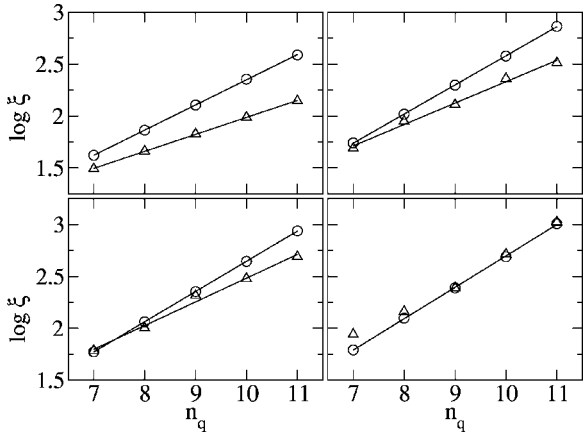


FIG. 4. IPR as a function of $N=2^{n_q}$ for column vectors (circles) and eigenvectors (triangles) of ISRM (nonsymmetric case), for $\alpha=1/3,1/5$ (top), and $\alpha=1/7,(1+\sqrt{5})/2$ (bottom). Data for column vectors are for 100 000th iterate. Straight lines show $\xi\propto N^{0.80},N^{0.93},N^{0.97},N^{1.00}$ (column vectors), and $\xi\propto N^{0.54},N^{0.69},N^{0.76},N^{1.00}$ (eigenvectors). Logarithms are decimal.

that for ISRM matrix element and $Q$ distributions converge to a limiting distribution which depends on $\alpha$. For irrational $\alpha$, the distribution corresponds to CUE predictions (even in the symmetric case where eigenvalue statistics follow COE, data not shown). For rational $\alpha$ where eigenvalue statistics follow semi-Poisson predictions, the limiting distributions are different from both COE and CUE distributions in $p$ representation (in $q$ representation they converge to CUE predictions, data not shown). Intermediate eigenvalue statistics are also usually associated with fractal properties of eigenvectors. This was observed in the Anderson model at the metal-insulator transition or in pseudointegrable systems. As was seen in [17], this is also the case for the ISRM. In a quantum information setting, randomly chosen eigenvectors of ISRM can be obtained by using the phase estimation algorithm and measuring an eigenvalue: the wave function collapses to the eigenvector associated to the eigenvalue measured. One can also easily obtain column vectors of ISRM by iterating a basis vector. In Fig. 4 we display the inverse participation ratio (IPR) for the eigenvectors and column vectors. This quantity is given by $\xi=\Sigma_i|\Psi_i|^2/\Sigma_i|\Psi_i|^4$ for a wave function $|\Psi\rangle=\Sigma_i\Psi_i|i\rangle$. It gives the number of basis states supporting the wave function ($\xi=1$ for a state localized on a single basis state, and $\xi=N$ for a state uniformly spread over $N$ of them). The results show that where intermediate statistics are present, for both eigenvectors and column vectors of ISRM one has $\xi\propto N^\gamma$ with $\gamma<1$, indicating fractal distributions of components. Such fractal properties may also depend on number-theoretic properties of $N$ (as is the case [23] for the baker's map). The precise investigation of such dependence requires more extensive studies.

In conclusion, we have shown that quantum maps displaying intermediate statistics can be simulated with a remarkable economy of resources on a quantum computer, especially in a NMR setting. We have also explored the link between such intermediate statistics, entangling power of the quantum evolution and matrix elements distribution. At last, we have shown that a suitably randomized map can be used as an efficient generator of pseudorandom operators displaying statistical properties different from RMT, and in particular producing fractal random vectors.

We thank K. Frahm for discussions, and CalMiP in Toulouse and IDRIS in Orsay for access to their supercomputers. This work was supported in part by the project EDIQIP of the IST-FET program of the EC.

[1] M. A. Nielsen and I. L. Chuang, *Quantum Computation and Quantum Information* (Cambridge University Press, Cambridge, England, 2000).
[2] S. Lloyd, Science **273**, 1073 (1996).
[3] R. Schack, Phys. Rev. A **57**, 1634 (1998).
[4] B. Georgeot and D. L. Shepelyansky, Phys. Rev. Lett. **86**, 2890 (2001).
[5] G. Benenti, G. Casati, S. Montangero, and D. L. Shepelyansky, Phys. Rev. Lett. **87**, 227901 (2001).
[6] Y. S. Weinstein, S. Lloyd, J. Emerson, and D. G. Cory, Phys. Rev. Lett. **89**, 157902 (2002).
[7] C. Miquel, J. P. Paz, M. Saraceno, E. Knill, R. Laflamme, and C. Negrevergne, Nature (London) **418**, 59 (2002); M. Terraneo, B. Georgeot, and D. L. Shepelyansky, Phys. Rev. E **71**, 066215 (2005).
[8] J. Emerson, Y. S. Weinstein, S. Lloyd, and D. G. Cory, Phys. Rev. Lett. **89**, 284102 (2002); D. Poulin, R. Blume-Kohout, R. Laflamme, and H. Ollivier *ibid.* **92**, 177906 (2004).
[9] D. Poulin, R. Laflamme, G. J. Milburn, and J. P. Paz, Phys. Rev. A **68**, 022302 (2003).
[10] G. Benenti, G. Casati, S. Montangero, and D. L. Shepelyansky Phys. Rev. A **67**, 052312 (2003).
[11] J. N. Bandyopadhyay and A. Lakshminarayan, Phys. Rev. Lett. **89**, 060402 (2003); A. Scott and C. Caves, J. Phys. A **36**, 9553 (2003).
[12] J. Emerson, Y. Weinstein, M. Saraceno, S. Lloyd, and D. Cory, Science **302**, 2098 (2003).
[13] B. I. Shklovskii, B. Shapiro, B. R. Sears, P. Lambrianides, and H. B. Shore, Phys. Rev. B **47**, 11487 (1993); D. Braun, G. Montambaux, and M. Pascaud, Phys. Rev. Lett. **81**, 1062 (1998).
[14] E. B. Bogomolny, U. Gerland, and C. Schmit, Phys. Rev. E **59**, R1315 (1999).
[15] E. Bogomolny, O. Giraud, and C. Schmit, Phys. Rev. E **65**, 056214 (2002).
[16] O. Giraud, J. Marklof, and S. O'Keefe, J. Phys. A **37**, L303 (2004).
[17] E. Bogomolny and C. Schmit, Phys. Rev. Lett. **93**, 254102 (2004).
[18] Y. S. Weinstein and C. S. Hellberg, Phys. Rev. Lett. **95**, 030501 (2005).
[19] K. M. Frahm, R. Fleckinger, and D. L. Shepelyansky, Eur. Phys. J. D **29**, 139 (2004); T. Gorin, T. Prosen, and T. H. Seligman, New J. Phys. **6**, 20 (2004).
[20] E. Knill and R. Laflamme, Phys. Rev. Lett. **81**, 5672 (1998).
[21] D. A. Meyer and N. R. Wallach, J. Math. Phys. **43**, 4273 (2002); G. K. Brennen, Quantum Inf. Comput. **3**, 619 (2003).
[22] M. Pozniak, K. Zyczkowski, and M. Kus, J. Phys. A **31**, 1059 (1998).
[23] N. Meenakshisundaram and A. Lakshminarayan, Phys. Rev. E **71**, 065303(R) (2005).